

Kepler map

B. Kaulakys* and G. Vilitis†

Institute of Theoretical Physics and Astronomy, A. Goštauto 12, 2600 Vilnius, Lithuania

Abstract

We present a consecutive derivation of mapping equations of motion for the one-dimensional classical hydrogenic atom in a monochromatic field of any frequency. We analyze this map in the case of high and low relative frequency of the field and transition from regular to chaotic behavior. We show that the map at aphelion is suitable for investigation of transition to chaotic behavior also in the low frequency field and even for adiabatic ionization when the strength of the external field is comparable with the Coulomb field. Moreover, the approximate analytical criterion (taking into account the electron's energy increase by the influence of the field) yields a threshold field strength quite close to the numerical results. We reveal that transition from adiabatic to chaotic ionization takes place when the ratio of the field frequency to the electron Kepler frequency approximately equals 0.1. For the dynamics and ionization in a very low frequency field the Kepler map can be converted to a differential equation and solved analytically. The threshold field of the adiabatic ionization obtained from the map is only 1.5% lower than the exact field strength of static field ionization.

PACS number(s): 05.45+b, 32.80.Rm, 42.50.Hz

* Electronic address: kaulakys@itpa.lt

† Electronic address: gedas@itpa.lt

1. INTRODUCTION

It is already the third decade when the highly excited hydrogen atom in a microwave field remains one of the simplest and most proper real system for experimental and theoretical investigation of classical and quantum chaos in the nonlinear systems strongly driven by external driving fields (see reviews [1–5] and references herein). For theoretical analysis of transition to stochastic behavior and ionization processes of atoms in microwave fields approximate mapping equations of motion, rather than differential equations, are most convenient.

Such a two-dimensional map (for the scaled energy of the one-dimensional atom in a monochromatic field and for the relative phase of the field), later called *Kepler map* [3,13], has been obtained in Refs. [6,7] after an integration of equations of motion for one period of the intrinsic motion of the electron between two subsequent passings of the aphelion, the largest distance from the nucleus. This map greatly facilitates numerical investigation of dynamics and ionization process and allows even an analytical estimation of the threshold field strengths for the onset of chaos, the diffusion coefficient of the electron in energy space and other characteristics of the system [3–10]. Moreover, this map is closely related to the expressions of quasiclassical dipole matrix elements for high atomic states [11,12].

The Kepler map for relatively high frequencies of the field (recovered in [3,13] and sometimes represented for the number of absorbed photons) is relatively simple and is widely used for analysis of classical dynamics, as well as after the quantization – the quantum Kepler map for the quantum dynamics [3–5,9,10,13]. In the region of relatively low frequency of the field this map is sufficiently more complex, the threshold field strength for transition to chaotic behavior and ionization is considerably higher than that for transition to chaotic behavior in the medium and high frequency fields.

Since derivation of the mapping equations of motion is based on the classical perturbation theory and the electron's energy change due to interaction with an external field during the period of motion in the Coulomb field depends on the initial condition, i.e., on the integration interval [6,7,11], complementary analysis of the applicability of the 'standard' Kepler map is necessary.

It should be noted, that in derivation of the Kepler map one integrates not over the period of the external electromagnetic field but over the period of the electron intrinsic motion in the Coulomb field [6,7]. This results in some contradictions and difficulties. First, the period of integration and the obtained map depend on the energy of the electron which complicates the quantization problem of the Kepler map [3–7,13–17]. Second, the energy change of the electron during the period of the classical intrinsic motion due to interaction with the microwave field depends on the starting conditions, i.e., on the integration interval [7,11]. This makes it possibility to obtain another map, the Kepler map at perihelion, derived by the integration between two subsequent passings of the perihelion [7] or even a three-dimensional map for the two halves of the intrinsic period [11]. These maps stronger reveal the resonance structure of chaotic dynamics at low frequencies [6,7,11,15].

Moreover, Nauenberg [18] has presented a so-called *canonical Kepler map* which agrees with the results of Refs. [6,7,11] if taken at perihelion but not with the widely used Kepler map at aphelion. The expressions for the variables of this canonical Kepler map are, however, sufficiently complicated, not explicit and, therefore, they are not comfortable for analytical and even numerical analysis. So, for this reason corroboration of the standard Kepler map's applicability for the large range of parameters of the problem is significant as well. Note additionally, that in derivation and analysis of the maps in Ref. [7] some inaccuracy and misprints have appeared.

All these aspects indicate the need of additional analysis of the mapping equations of motion for a highly excited classical hydrogenic atom in a monochromatic field. In addition, transition from adiabatic to chaotic ionization mechanism in the a frequency field is of great interest (see, e.g. [19] and references herein).

In this paper we present a consistent derivation of the mapping equations of motion for a one-dimensional classical atom in a monochromatic field of any frequency and analyze transition from regular to chaotic behavior and ionization process. From the fulfilled analysis we conclude that the map at aphelion and an approximate analytical criterion of the onset of chaos are suitable also in the low frequency region, even for adiabatic ionization, where the strength of the external field is comparable with the Coulomb field. Moreover, in this case the map can be transformed to a differential equation and solved analytically.

2. MAPPING EQUATIONS OF MOTION

The direct way of coupling the electromagnetic field to the electron Hamiltonian is through the $\mathbf{A} \cdot \mathbf{P}$ interaction, where \mathbf{A} is the vector potential of the field and \mathbf{P} is the generalized momentum of the electron. The Hamiltonian of the hydrogen atom in a linearly polarized field $F \cos(\omega t + \vartheta)$, with F , ω and ϑ being the field strength amplitude, field frequency and phase, respectively, in atomic units is

$$H = \frac{1}{2} \left(\mathbf{P} - \frac{\mathbf{F}}{\omega} \sin(\omega t + \vartheta) \right)^2 - \frac{1}{r}. \quad (1)$$

The electron energy change due to interaction with the external field follows from the Hamiltonian equations of motion [20]

$$\dot{E} = -\dot{\mathbf{r}} \cdot \mathbf{F} \cos(\omega t + \vartheta). \quad (2)$$

Note, that Eq. (2) is exact if $\dot{\mathbf{r}}$ is obtained from equations of motion including influence of the electromagnetic field. Using parametric equations of motion in the Coulomb field we can calculate the change of the electron's energy in the classical perturbation theory approximation [6–8,11].

Measuring the time of the field action in the field periods one can introduce the scale transformation [16,18] where the scaled field strength and the scaled energy are $F_s = F/\omega^{4/3}$ and $E_s = E/\omega^{2/3}$, respectively. However, it is convenient [6–8,17] to introduce the positive scaled energy $\varepsilon = -2E_s$ and the relative field strength $F_0 = Fn_0^4 = F_s/\varepsilon_0^2$, with n_0 being the initial effective principle quantum number, $n_0 = (-2E_0)^{-1/2}$. The threshold values of the relative field strength F_0 for the ionization onset depends weaker upon the initial effective principle quantum number n_0 and the relative frequency of the field $s_0 = \omega n_0^3$ than the scaled field strength F_s .

We restrict our subsequent consideration to the one-dimensional model, which corresponds to states very extended along the electric field direction. Such classical one-dimensional model was first considered in Refs. [21] for the description of surface-state electrons, while a justification of the use of one-dimensional-like states for periodically driven hydrogen atoms appeared in [22]. Since that the one-dimensional model is widely used in theoretical analysis [2–11,13–17].

For the derivation of a map describing the motion of an electron in the superposition of the Coulomb and microwave fields we should integrate dynamical equations over some characteristic period of the system. The peculiarity of the system under consideration is that we are able to obtain explicit expressions for the change of the electron energy only for halves of the period and for the complete period, $T = 2\pi/(-2E)^{3/2} = 2\pi/\omega\varepsilon^{3/2}$, of the intrinsic electron motion in the Coulomb field [6–8,11] but not for the period of the external field.

Integration of Eq. (2) for motion between two subsequent passages at the aphelion (where $\dot{x} = 0$ and there is no energy exchange between the field and the atom) results in the change of the electron's energy [6,7,11]

$$\Delta E = -(\pi F/E) \mathbf{J}'_s(s) \sin \vartheta.$$

Here $s \equiv \varepsilon^{-3/2} = \omega/(-2E)^{3/2} = \omega/\Omega$ is the relative frequency of the field, i.e., the ratio of the field frequency ω to the Kepler orbital frequency $\Omega = (-2E)^{3/2}$, and $\mathbf{J}'_s(z)$ is the derivative of the Anger function with respect to the argument z . The derivative of the Anger function

$$\mathbf{J}'_s(s) = \frac{1}{\pi} \int_0^\pi \sin[s(x - \sin x)] \sin x dx$$

is a very simple analytical function which can be approximated quite well by some combination [7] of expansion in powers of s

$$\mathbf{J}'_s(s) = \frac{1 + (5/24)s^2}{2\pi(1 - s^2)} \sin \pi s, \quad s \leq 1$$

and of the asymptotic form

$$\mathbf{J}'_s(s) = \frac{b}{s^{2/3}} - \frac{a}{5s^{4/3}} - \frac{\sin \pi s}{4\pi s^2}, \quad s \gg 1$$

where

$$a = \frac{2^{1/3}}{3^{2/3}\Gamma(2/3)} \simeq 0.4473, \quad b = \frac{2^{2/3}}{3^{1/3}\Gamma(1/3)} \simeq 0.41085.$$

Introducing the scaled energy $\varepsilon = -2E/\omega^{2/3}$ and the relative field strength $F_0 = F/4E_0^2$ we have

$$\Delta \varepsilon = -\pi F_0 \varepsilon_0^2 h(\varepsilon) \sin \vartheta \quad (3)$$

where $\varepsilon_0 = -2E_0/\omega^{2/3}$ and

$$h(\varepsilon) = \frac{4}{\varepsilon} \mathbf{J}'_s(s). \quad (4)$$

The change of the field phase ϑ after the electron motion period in the Coulomb field is

$$\Delta \vartheta = 2\pi \omega T = 2\pi/\varepsilon^{3/2}. \quad (5)$$

Defining the scaled energy and the phase before, $\varepsilon_j, \vartheta_j$, and after, $\varepsilon_{j+1}, \vartheta_{j+1}$, passages of the electron of one intrinsic motion period we can introduce [23,24] a generating function $G(\varepsilon_{j+1}, \vartheta_j)$ of the map determined as

$$\varepsilon_j = \partial G / \partial \vartheta_j, \quad \vartheta_{j+1} = \partial G / \partial \varepsilon_{j+1}. \quad (6)$$

In agreement with Eqs. (3) and (5) the generating function is (see also [3] for analogy)

$$G(\varepsilon_{j+1}, \vartheta_j) = \varepsilon_{j+1} \vartheta_j - 4\pi \varepsilon_{j+1}^{-1/2} - \pi F_0 \varepsilon_0^2 h(\varepsilon_{j+1}) \cos \vartheta_j \quad (7)$$

and according to Eqs. (6) it generates the map

$$\begin{cases} \varepsilon_{j+1} = \varepsilon_j - \pi F_0 \varepsilon_0^2 h(\varepsilon_{j+1}) \sin \vartheta_j, \\ \vartheta_{j+1} = \vartheta_j + 2\pi/\varepsilon_{j+1}^{3/2} - \pi F_0 \varepsilon_0^2 h(\varepsilon_{j+1}) \cos \vartheta_j. \end{cases} \quad (8)$$

Here

$$\eta(\varepsilon) = \frac{dh(\varepsilon)}{d\varepsilon}. \quad (9)$$

Note that the map (8) can be derived also without introduction of the generating function [6–8,11] but using the requirement of the area-preserving of the map (8) defined as

$$\frac{\partial(\varepsilon_{j+1}, \vartheta_{j+1})}{\partial(\varepsilon_j, \vartheta_j)} = 1. \quad (10)$$

It should also be noted that the map (14)-(19) in Ref. [7] is with the positive signs of terms in the right-hand site of Eq. (8) containing the field amplitudes F_0 , i.e., it is derived for the reverse orientation of the atom with respect to the field orientation. Also note that a function $\sin \vartheta_k$ was inadvertently omitted from the right-hand side of Eq. (15) in [7].

The map (8) is the general mapping form of the classical equations of motion for the one-dimensional hydrogen atom in a microwave field derived in the classical perturbation theory approximation. Some analytical and numerical analysis of this map has already been done in Refs. [3,6–8]. Here we analyze different special cases of the map (8).

3. HIGH FREQUENCY LIMIT

For relatively high frequencies of the field, $s \gg 1$ ($s \geq 2$), theoretical analysis of the classical dynamics of the one-dimensional hydrogen atom in a microwave field is relatively simple. That is why the energy changes of the electron, $(E_{j+1} - E_j)$ and $(\varepsilon_{j+1} - \varepsilon_j)$, do not depend on the initial energy ε_j and relative frequency $s \gg 1$. Indeed, using the asymptotic form of the derivative of the Anger function, $\mathbf{J}'_s(s) = b/s^{2/3}$, we have $h(\varepsilon_{j+1}) = 4b = \text{const.}$, $\eta(\varepsilon_{j+1}) = 0$ and, consequently, the following map

$$\begin{cases} \varepsilon_{j+1} = \varepsilon_j - 4\pi b F_0 \varepsilon_0^2 \sin \vartheta_j, \\ \vartheta_{j+1} = \vartheta_j + 2\pi/\varepsilon_{j+1}^{3/2}. \end{cases} \quad (11)$$

Note, that scaled classical dynamics according to maps (8) and (11) depends only on single combination of the field parameters, i.e., on the scaled field strength $F_s = F_0 \varepsilon_0^2 = F/\omega^{4/3}$ (see also [16,17]).

By the standard [23,24] linearization procedure, $\varepsilon_j = \varepsilon_0 + \Delta\varepsilon_j$, in the vicinity of the integer relative frequency (resonance), $s_0 = \varepsilon_0^{-3/2} = m$ with m integer, the map (11) can be transformed to the standard (Chirikov) map

$$\begin{aligned} I_{j+1} &= I_j + K \sin \vartheta_j, \\ \vartheta_{j+1} &= \vartheta_j + I_{j+1}. \end{aligned} \quad (12)$$

Here $I_j = -3\pi\Delta\varepsilon_j/\varepsilon_0^{5/2}$ and $K = 12\pi^2 b F_0/\sqrt{\varepsilon_0}$.

From the condition of the onset of classical chaos for the standard map, $K \geq K_c \simeq 0.9816$ [1,23–25], we can, therefore, estimate the threshold field strength for chaotization of dynamics and ionization of the atom in the high frequency field

$$F_0^c = K_c / (12\pi^2 b s_0^{1/3}) \simeq 0.02 s_0^{-1/3}. \quad (13)$$

Sometimes one writes the map (11) for a variable $N = -1/2n^2\omega$, which change gives the number of absorbed photons [3,13],

$$N_{j+1} = N_j + 2\pi \left(F/\omega^{5/3} \right) \sin \vartheta_j,$$

$$\vartheta_{j+1} = \vartheta_j + 2\pi\omega (-2\omega N_{j+1})^{-3/2}. \quad (14)$$

We see that for such variables the dynamics of the system depends on *two* parameters: on the ratio $F_q = F/\omega^{5/3}$ (in Refs. [16,17] $F_q = F/\omega^{5/3}$ was called the *quantum scaled field strength*) and on the field frequency ω . Map (14) is, therefore, not the most convenient one for analysis of the *classical* dynamics.

In general there are, however, no essential difficulties in the theoretical analysis of classical nonlinear dynamics of the highly excited hydrogen atom in the microwave field of relative frequency $s_0 = \omega n_0^3 \geq 0.5$ when the field strength is lower or comparable with the threshold field strength for the onset of classical chaos, i.e., if the microwave field is considerably weaker than the characteristic Coulomb field. In such a case, the energy change of the electron during the period of intrinsic motion is relatively small and application of the classical perturbation theory for derivation of the Kepler map (8) is sufficiently correct. Further analysis of transition to chaotic behavior and of the ionization process can be based on the map (8) and for $s_0 \simeq 0.3 \div 1.5$ results in the "impressive agreement" [5] between measured ionization curves and those obtained from the map (8) [5–10]. Even analytical estimation of the threshold field strengths based on this map is rather proper [6–8].

Considerably more complicated is the analysis of transition to stochastic motion and of ionization process in the region of low relative frequencies, $s_0 \leq 0.3$, [6–8,11].

4. LOW FREQUENCY LIMIT

For the low relative frequencies of the microwave field, $s \ll 1$, the map (8) can be simplified as well. Using expansion of the function $\mathbf{J}'_s(s)$ in powers of s , $\mathbf{J}'_s(s) \simeq s/2$, for $s \ll 1$ we have according to Eqs. (4) and (9)

$$\begin{aligned} h(\varepsilon_{j+1}) &= 2/\varepsilon_{j+1}^{5/2}, \\ \eta(\varepsilon_{j+1}) &= -5/\varepsilon_{j+1}^{7/2}. \end{aligned} \quad (15)$$

Consequently map (8) transforms to the form

$$\begin{cases} \varepsilon_{j+1} = \varepsilon_j - 2\pi F_0 \left(\varepsilon_0^2 / \varepsilon_{j+1}^{5/2} \right) \sin \vartheta_j, \\ \vartheta_{j+1} = \vartheta_j + 2\pi / \varepsilon_{j+1}^{3/2} + 5\pi F_0 \left(\varepsilon_0^2 / \varepsilon_{j+1}^{7/2} \right) \cos \vartheta_j. \end{cases} \quad (16)$$

This map is slightly more complicated than map (11) for high frequencies, however, it can easily be analyzed numerically as well as analytically. Note first of all, that the energy change of the electron during the period of intrinsic motion (after one step of iteration), $|\varepsilon_{j+1} - \varepsilon_j|$, is considerably smaller than the binding energy of the electron $\varepsilon_j \simeq \varepsilon_0$ if the field strength is lower or comparable with the threshold field strength, i.e., $2\pi F_0 \left(\varepsilon_0^2 / \varepsilon_{j+1}^{5/2} \right) \simeq 2\pi F_0 \varepsilon_0^{-1/2} \ll \varepsilon_0$, or $2\pi F_0 s_0 \ll 1$ if $F_0 \leq F_0^{st} \simeq 0.13$ and $s_0 \ll 1$. This indicates that the map (16) is probably suitable for description of dynamics even in the low frequency region where the field is relatively strong.

In Figs 1 and 2 the results of the numerical analysis of maps (8) and (16) in the low frequency, $s \leq 1$, area are presented. We see that the threshold ionization field calculated from the maps approaches the static field ionization threshold $F_0^{st} \simeq 0.13$ when $s_0 \rightarrow 0$. This supports the presumption that the map (8) is valid even in the low frequency limit where the strength of the driving field is of the order of the Coulomb field.

4.1. Adiabatic ionization

For low frequencies, $2\pi s = 2\pi/\varepsilon^{3/2} \ll 1$, according to the second equation of map (16) the change of the angle ϑ after one step of iteration is small. As it was noticed above, the energy

change is also relatively small. Therefore, we can transform the difference equations (16) to differential equations of the form

$$\begin{aligned}\frac{d\varepsilon}{dj} &= -\frac{2\pi\varepsilon_0^2 F_0}{\varepsilon^{5/2}} \sin \vartheta, \\ \frac{d\vartheta}{dj} &= \frac{2\pi}{\varepsilon^{3/2}} + \frac{5\pi\varepsilon_0^2 F_0}{\varepsilon^{7/2}} \cos \vartheta.\end{aligned}\tag{17}$$

Dividing second equation of the system (17) by the first one we obtain one differential equation

$$\frac{d(\cos \vartheta)}{d\varepsilon} = \frac{\varepsilon}{\varepsilon_0^2 F_0} + \frac{5 \cos \vartheta}{2\varepsilon}.\tag{18}$$

The analytical solution of Eq. (18) with the initial condition $\varepsilon = \varepsilon_0$ when $\vartheta = \vartheta_0$ is

$$\cos \vartheta = z^5 \cos \vartheta_0 - 2z^4 (1 - z) / F_0, \quad z = \sqrt{\varepsilon / \varepsilon_0}.\tag{19}$$

Eq. (16) describes the motion of the system in ε and ϑ variables, i.e., represents the functional interdependence between two dynamical variables.

Let us analyze Eqs. (18) and (19) in more detail. For relatively low values of F_0 , i.e., for $F_0 < \frac{2}{5}z^4 = \frac{2}{5}\left(\frac{\varepsilon}{\varepsilon_0}\right)^2$, the right-hand side of Eq. (18) is positive for all phases ϑ . Therefore, $\cos \vartheta$ and ε decrease and increase simultaneously and, according to Eq. (16), there is a motion in the whole interval $[0, 2\pi]$ of the angle ϑ . For $F_0 > \frac{2}{5}z^4$, however, the increase of the angle ϑ in the interval $0 \div \pi$ goes to decrease of ϑ at $\vartheta \simeq \pi$. This results in fast decrease of ε and to the ionization process (see also Fig. 1). It is easy to understand from analysis of Eq. (19) that the minimal value of F_0 for such a motion (resulting in ionization) corresponds to $\vartheta_0 = 0$ and $\vartheta = \pi$. This value of F_0 is very close to the maximal value of F_0 resulting from motion in the whole interval $[0, 2\pi]$ of ϑ , i.e., the maximum of the expression

$$F_0 = 2z(1 - z) / (1 + z^5).\tag{20}$$

This maximum is at $z = z_0$, where z_0 is a solution of the equation $z^5 + 5z - 4 = 0$, being $z_0 \simeq 0.75193$. The critical value of the relative field strength, therefore, is $F_0^c = 2z_0^4/5 = 0.1279$ which is only 1.5% lower than the adiabatic ionization threshold $F_0^{st} = 2^{10}/(3\pi)^4 = 0.1298$ [7,21]. According to our numerical analysis, if $s_0 \leq 0.05$ the electron remains bounded and the dynamics is regular for $F_0 \leq 0.13$ while ionization takes place for $F_0 \geq 0.131$ (see also Fig. 1 and 2). These results are very close as well to analytical conclusions. Note, that some decrease of the threshold field strength values F_0^c with decreasing of s_0 was observed for $s_0 \leq 0.1$. Dynamics and classical ionization at such frequencies are, however, essentially adiabatic.

4.2. Chaotic ionization

For higher relative frequencies, $s_0 \geq 0.1$, ionization process is due to chaotic dynamics of the highly excited electron of the hydrogenic atom in a microwave field. There are different criterions for estimation of the parameters when the dynamics of the nonlinear system becomes chaotic. For analysis of transition to chaotic behavior of the motion described by maps (8), (11) and (16) the most proper, to our mind, is the criterion related with the randomization of the phases [24]

$$K = \max \left| \frac{\delta \vartheta_{j+1}}{\delta \vartheta_j} - 1 \right| \geq 1.\tag{21}$$

Here max means the maximum with respect to the phase ϑ_j and variation of the phase ϑ_{j+1} with respect to the phase ϑ_j means the full variation including dependence of ϑ_{j+1} on ϑ_j through the variable ε_{j+1} in Eqs. (8), (11) and (16).

Applying criterion (21) to the general map (8) we obtain the threshold field strength

$$F_0^c = \frac{\varepsilon^{7/2}}{12\pi^2 \varepsilon_0^2 \mathbf{J}'_s(s)}. \quad (22)$$

If $\varepsilon \simeq \varepsilon_0$ Eq. (22) yields the result

$$F_0^c = \left(12\pi^2 s \mathbf{J}'_s(s)\right)^{-1} \quad (23)$$

which for $s \gg 1$ coincides with Eq. (13).

For more precise evaluation of the critical field strengths we should take into account the change (increase) of the electron's energy due to the influence of the electromagnetic field. For higher relative frequency s or lower scaled energy ε_j the threshold ionization field is lower. Therefore, if the scaled energy ε_j decreases as a result of relatively regular dynamics in a not very strong microwave field, then the lower field strength is sufficient for transition to chaotic dynamics. For high frequencies such change of the energy is relatively small. Nevertheless it reveals some resonance structure in the field-atom interaction. In the low frequency limit the energy change is more essential. Now consider it in detail.

As it was shown above, maximal decrease of the scaled energy ε_j is for the angle $\vartheta_j \simeq \pi$ and it can be evaluated from Eq. (20). Taking this into account we have from Eq. (16) according to criterion (21) the expression for the threshold relative field strength

$$F_0^c = \frac{\varepsilon^5}{6\pi^2 \varepsilon_0^2} = \frac{z_c^{10}}{6\pi^2 s_0^2} \quad (24)$$

where z_c is the solution of Eq. (20) with $F_0 = F_0^c$. Eq. (20) can be solved approximately expanding z_c^{10} in powers of F_0^c . The result of such an expansion is

$$z_c^{10} \simeq 1 - 10F_0^c + 30(F_0^c)^2 - 73.6(F_0^c)^3 \quad (25)$$

where the last term in the right-hand side of Eq. (25) is from the requirement of the exact maximal value $z_c = z_0 = 0.75193$ for the static threshold field strength $F_0^c = 0.1279$.

For evaluation of the threshold field for transition to chaotic behavior in the low frequency field we should thus solve the system of equations (24) and (25). For $0.09 \leq s_0 \leq 0.5$ expressions (24) and (25) give an ionization threshold field very close to the numerical results (see Fig. 2). For frequencies lower than $s_0 \simeq 0.09$ ionization is adiabatic, because for so low frequencies the adiabatic ionization threshold field, $F_0^c = 2z_0^4/5 = 0.1279$, is lower than the phase randomization field evaluated according to Eqs. (24) and (25). The adiabatic ionization, therefore, occurs in such a case earlier than the chaotization of the dynamics. Note, that numerical results reveal transition from adiabatic to chaotic ionization at relative frequency $s_0 \simeq 0.1$ (scaled energy $\varepsilon_0 \simeq 4.3$) as well.

At higher frequencies ionization is due to chaotic dynamics while transition to chaotic behavior can be evaluated from the approximate criterion (21) taking into account the electron's energy change by the influence of the electromagnetic field. For frequencies higher than $s_0 \simeq 0.5$ we should use a more exact expression than $\mathbf{J}'_s(s) \simeq s/2$ for the derivative of the Anger function, i.e., Eq. (22).

5. CONCLUDING REMARKS

From the analysis given in this study we can conclude that the map at aphelion (8) is suitable for investigation of regular and stochastic classical dynamics, transition to chaotic behavior and ionization of Rydberg atoms in high, medium and low frequency fields, even for adiabatic ionization when the strength of the external field is comparable with the averaged Coulomb field. For such a purpose it is unnecessary to use the map at perihelion, the map for two halves of the intrinsic period or the canonical Kepler map [7,11,18]. Moreover, the approximate criterion (21) for transition to chaotic behavior yields a threshold field strength very close to the numerical results if we take into account increase of the electron energy by influence of the electromagnetic field. Transition from adiabatic to chaotic ionization of the classical hydrogenic atom in a monochromatic field takes place at a relative field frequency $s_0 \simeq 0.1$.

Furthermore, the Kepler map and some generalizations of it (for two- and multi-frequency [9,10,26] or some other fields, e.g., circular polarized microwave field, for three-dimensional atoms and other modifications) are and may be more widely used for analysis of different effects of classical and quantum chaos in driven nonlinear systems [19,27,28]. Note also the attempts to derive and use similar maps in astronomy for analysis of chaotic dynamics of comets and other astronomical bodies [29]. It turns out, however, that in such a case, generalization of the Kepler map for nonharmonic perturbations and for motion in three-dimensional space, is necessary.

ACKNOWLEDGMENT

The research described in this publication was made possible in part by support of the Alexander von Humboldt Foundation.

References

1. Delone, N. B., Krainov, V. P. and Shepelyansky, D. L., Usp. Fiz. Nauk **140**, 355 (1983) [Sov. Phys.-Usp. **26**, 551 (1983)].
2. Casati, G., Chirikov, B. V., Shepelyansky, D. L. and Guarneri, I., Phys. Rep. **154**, 77 (1987).
3. Casati, G., Guarneri, I. and Shepelyansky, D. L., IEEE J. Quantum Electron. **24**, 1420 (1988).
4. Jensen, R. V., Susskind, S. M. and Sanders, M. M., Phys. Rep. **201**, 1 (1991).
5. Koch, P. M., in "Chaos and Quantum Chaos", edited by Heiss, W. (Lecture Notes in Physics Vol. **411**, Springer-Verlag, Berlin, 1992), p. 167; Koch, P. M. and van Leeuwen, K. A. H., Phys. Rep. **255**, 289 (1995).
6. Gontis, V. and Kaulakys, B., Deposited in VINITI as No.5087-V86 (1986) and Lit. Fiz. Sb. **27**, 368 (1987) [Sov Phys.-Collect. **27**, 111 (1987)].
7. Gontis, V. and Kaulakys, B., J. Phys. B: At. Mol. Opt. Phys. **20**, 5051 (1987).
8. Kaulakys, B. and Vilutis, G., in "Chaos - The Interplay between Stochastic and Deterministic Behaviour", edited by Garbaczewski, P., Wolf, M. and Weron, A. (Lecture Notes in Physics Vol. **457**, Springer-Verlag, Berlin, 1995), p. 445; chao-dyn/9503011.

9. Moorman, L., Galvez, E. J., Sauer, B. E., Mortazawi-M., A., van Leeuwen, K. A. H., v.Oppen, G. and Koch, P. M., Phys. Rev. Lett. **61**, 771 (1988); Galvez, E. J., Sauer, B. E., Moorman, L., Koch, P. M. and Richards, D., Phys. Rev. Lett. **61**, 2011 (1988); Koch, P. M., Moorman, L., Sauer, B. E., Galvez, E. J. and Leeuwe, K. A. H., Phys. Scripta **T26**, 51 (1989); Haffmans, A., Blümel, R., Koch, P. M. and Sirko, L., Phys. Rev. Lett. **73**, 248 (1994).
10. Siko, L. and Koch, P. M., Appl. Phys. B **60**, S195 (1995); Koch, P. M., Physica D **83**, 178 (1995).
11. Kaulakys, B., J. Phys. B: At. Mol. Opt. Phys. **24**, 571 (1991).
12. Kaulakys, B., J. Phys. B: At. Mol. Opt. Phys. **28**, 4963 (1995); physics/9610018.
13. Casati, G., Guarneri, I. and Shepelyansky, D. L., Phys. Rev. A **36**, 3501 (1987).
14. Graham, R., Europhys. Lett. **7**, 671 (1988); Leopold, J. G. and Richards, D., J. Phys. B: At. Mol. Opt. Phys. **23**, 2911 (1990).
15. Gontis, V. and Kaulakys, B., Lit. Fiz. Sb. **28**, 671 (1988) [Sov. Phys. - Collec. **28** (6), 1 (1988)]; Gontis V. and Kaulakys, B., Lit. Fiz. Sb. **31**, 128 (1991) [Lithuanian Phys. J. (Allerton Press, Inc.) **31** (2), 75 (1991)]
16. Kaulakys, B., Gontis, V., Hermann, G. and Scharmann, A., Phys. Lett. A **159**, 261 (1991); Kaulakys, B., Acta Phys. Pol. B **23**, 313 (1992).
17. Kaulakys, B., Gontis, V. and Vilutis, G., Lith. Phys. J. (Allerton Press, Inc.) **33**, 290 (1993); Kaulakys, B. and Vilutis, G., in *AIP Conf. Proc.* (AIP, New York) **329**, 389 (1995); quant-ph/9504007.
18. Nauenberg, M., Europhys. Lett. **13**, 611 (1990).
19. Blümel, R., Phys. Rev. A **49**, 4787 (1994); Sundaram, B. and Jensen, R. V., Phys. Rev. A **51**, 4018 (1995); Koch, P. M., Acta Phys. Pol. A **93**, 105 (1998).
20. Landau, L. D. and Lifshitz, E. M., "Classical Field Theory" (Pergamon, New York, 1975).
21. Jensen, R. V., Phys. Rev. Lett. **49**, 1365 (1982); Phys. Rev. A **30**, 386 (1984).
22. Shepelyansky, D. L., in *Proc. Intern. Conf. on Quantum Chaos*, Como, 1983 (Plenum, New York, 1995), p. 187.
23. Lichtenberg, A. J. and Lieberman, M. A., "Regular and Stochastic Motion" (Springer-Verlag, New York, 1983 and 1992).
24. Zaslavskii, G. M., "Stochastic Behavior of Dynamical Systems" (Nauka, Moscow, 1984; Harwood, New York, 1985).
25. Jensen, R. V., Am. Scient. **75**, 168 (1987).
26. Howard, J. E., Phys. Lett. A **156**, 286 (1991); Kaulakys, B., Grauzhins, D. and Vilutis, G., Europhys. Lett. **43**, 123 (1998); physics/9808048.

27. Casati, G., Guarneri, I. and Mantica, G., Phys. Rev. A **50**, 5018 (1994); Buchleitner, A., Delande, D., Zakrzewski, J., Mantenga, R. N., Arndt, M. and Walther, H., Phys. Rev. Lett. **75**, 3818 (1995); Wojcik, M., Zakrzewski, J. and Rzazewski, K., Phys. Rev. A **52**, 2523 (1995); Sanders, M. M. and Jensen, R. V., Am. J. Phys. **64**, 21 and 1013 (1996); Sacha, K. and Zakrzewski, J., Phys. Rev. A **55**, 568 (1997).
28. Jensen, R. V., Nature (London) **355**, 311 (1992); Sirko, L., Haffmans, A., Bellermand, M. R. W. and Koch, P. M., Europhys. Lett. **33**, 181 (1996); Brenner, N. and Fishman, S., Phys. Rev. Lett. **77**, 3763 (1996) and J. Phys. A **29**, 7199 (1996); Benvenuto, F., Casati, G. and Shepelyansky, D. L., Phys. Rev. A **55**, 1732 (1997); Buchleitner, A. and Delande, D., Phys. Rev. A **55**, 1585 (1997).
29. Petrosky, T. Y., Phys. Lett. A **117**, 328, (1986); Sagdeev, R. Z. and Zaslavsky, G. M., Nouvo. Cim. B **97**, 119 (1987); Chirikov, B. V. and Vecheslavov, V. V., Astron. Astrophys. **221**, 146 (1989); Torbett, V. M. and Smoluchowski, R., Nature (London) **345**, 49 (1990); Milani, A. and Nobili, A. M., Nature (London) **357**, 569 (1992); Chicone, C. and Retzloff, D. G., J. Math. Phys. **37**, 3997 (1996).

Caption for the figures

Fig. 1. Trajectories of the map (8) for different initial conditions, ε_0, θ_0 , and different relative field strength F_0 . The pictures in the left-hand side correspond to the regular quasiperiodic motion while those in the right-hand side represent ionization process for a little stronger field. At $\varepsilon_0 \simeq 4.3$, i.e., $s_0 \simeq 0.11$ a transition from the adiabatic to the chaotic ionization mechanism takes place.

Fig. 2. Relative threshold field strength for the onset of ionization from numerical analysis of the maps (8) and (16) and according to the approximate criterion (24) - (25).

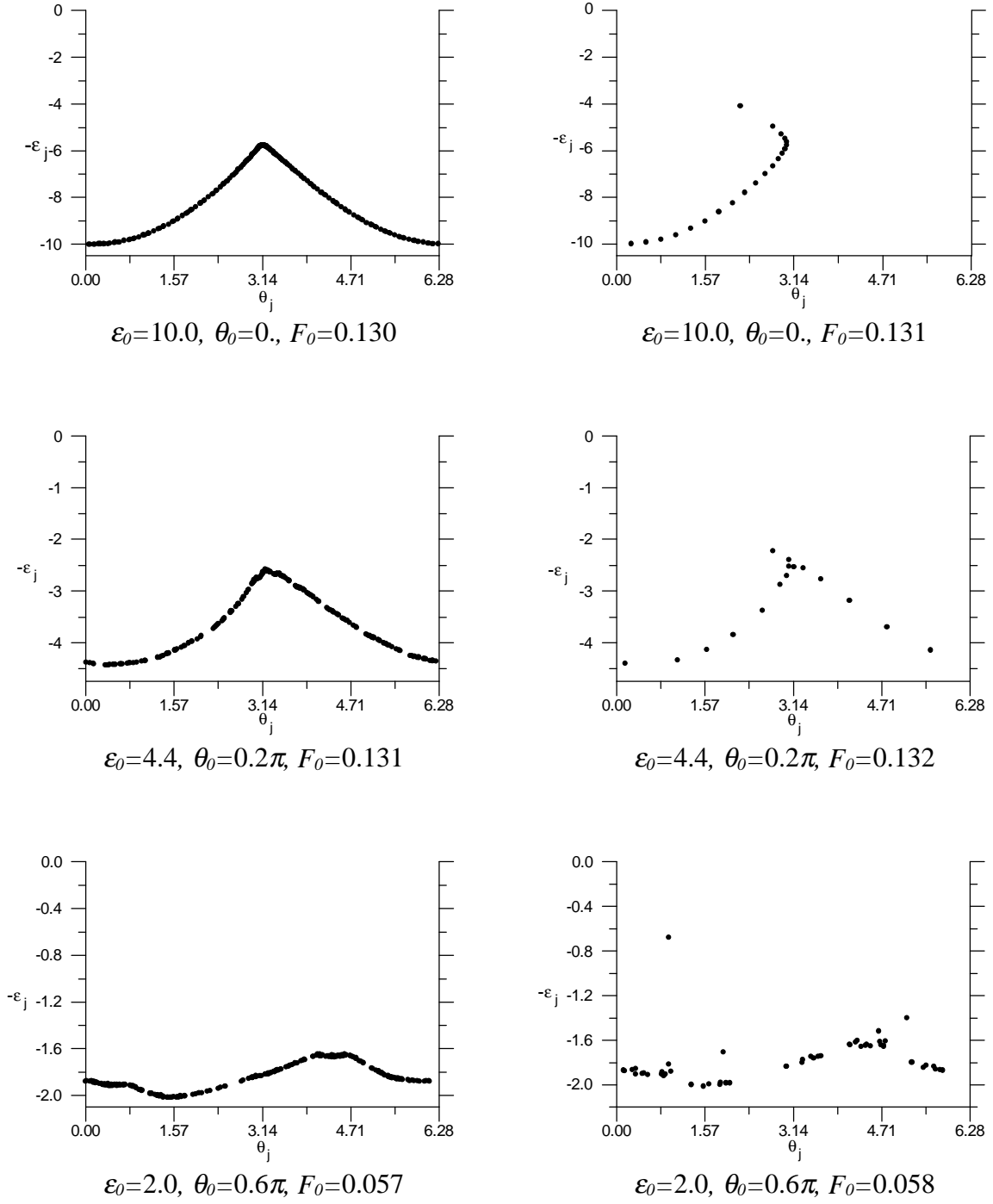


Fig. 1. Trajectories of the map (8) for different initial conditions, ε_0, θ_0 , and different relative field strength F_0 . The pictures in the left-hand side correspond to the regular quasiperiodic motion while those in the right-hand side represent ionization process for a little stronger field. At $\varepsilon_0 \approx 4.3$, i.e., a $s_0 \approx 0.11$ a transition from the adiabatic to the chaotic ionization mechanism takes place.

